

Thermal annealing effects on the structural and electrical properties of $\text{HfO}_2/\text{Al}_2\text{O}_3$ gate dielectric stacks grown by atomic layer deposition on Si substrates

Moonju Cho, Hong Bae Park, Jaehoo Park, and Cheol Seong Hwang^{a)}
*School of Materials Science and Engineering and Interuniversity Semiconductor Research Center,
Seoul National University, Seoul 151-742, Korea*

Jong-Cheol Lee and Se-Jung Oh
*School of Physics and Center for Strongly Correlated Materials Research, Seoul National University,
Seoul 151-742, Korea*

Jaehack Jeong and Kwang Soo Hyun
*Ever-tek Company, 401 Hyundai I-belly, 223-12 Sangdeawon-dong, Jungwon-ku Sunnam,
Kyunggi-do 462-120 Korea*

Hee-Sung Kang, Young-Wuk Kim, and Jong-Ho Lee
*System LSI, Semiconductor Business, Samsung Electronics Company, Limited, Kiheung, Kyunggi-do 449-
711, Korea*

(Received 21 February 2003; accepted 19 May 2003)

$\text{HfO}_2/\text{Al}_2\text{O}_3$ gate dielectric thin film stacks were deposited on Si wafers using the atomic layer deposition technique. A 3.3-nm-thick Al_2O_3 interlayer was grown at 400 °C using $\text{Al}(\text{CH}_3)_3$ and O_3 , and 2.5–3.5-nm-thick HfO_2 films were grown at either 300 or 400 °C using HfCl_4 and H_2O . Thermal annealing of the dielectric film stack at temperatures ranging from 400 to 1000 °C under pure N_2 atmosphere resulted in variation of the equivalent oxide thicknesses. The equivalent oxide thickness of the dielectric film stack showed a minimum after annealing at 650 °C irrespective of the HfO_2 film growth temperature. High temperature (>800 °C) annealing induced the formation of SiO_2 and intermixing between the HfO_2 and Al_2O_3 layers, which resulted in an increase in the equivalent oxide thickness of the film stack. The structural changes in the stacked films as a function of the annealing temperature were compared with those of HfO_2 and Al_2O_3 single layers. The film stack showed minimal hysteresis (<15 mV) behavior in the capacitance–voltage curve and a shift in flat-band voltage of 0.6–0.9 V by negative fixed charges at the $\text{Al}_2\text{O}_3/\text{SiO}_2$ interface after annealing at temperature >500 °C. The variation in fixed charge density as a function of the annealing temperature was also investigated. A minimum equivalent oxide thickness of 1.3 nm with leakage current density of 8×10^{-6} A/cm² at –1 V was obtained with the poly-Si electrode even after annealing at 1000 °C for 10 s. This leakage current density is seven orders of magnitude smaller than that of SiO_2 with similar equivalent oxide thickness. © 2003 American Institute of Physics. [DOI: 10.1063/1.1590414]

I. INTRODUCTION

Among the many candidate materials, HfO_2 has recently been highlighted^{1–4} as a replacement for nitrided SiO_2 gate oxide films used in complementary metal–oxide–semiconductor (CMOS) devices due to its reasonably high dielectric constant (>20), thermodynamic compatibility of the interface with Si, gate poly-Si compatibility, and relatively large band gap (5.68 eV). However, most vapor phase grown HfO_2 thin films appear to have interfacial layers (ILs) at the Si interface due to the presence of excess oxidizing elements and concurrent Si diffusion into the growing films. This reduces the overall capacitance density, and should therefore be minimized in order to realize high- k characteristics. It should be noted that high temperature (~1050 °C, 10 s) postannealing is inevitable for current CMOS fabrication processes. During postannealing, high- k films are usu-

ally affected both structurally and electrically. We recently reported that HfO_2 films grown directly on a Si wafer either by chemical vapor deposition (CVD) or by atomic layer deposition (ALD) suffered from these problems.^{5,6} Therefore, it was concluded that a certain reaction barrier layer (RBL) placed between the HfO_2 film and Si substrate is essential for obtaining smaller equivalent oxide thickness (EOT) values. There are several other electrical parameters that ought to be taken into consideration, such as the shift in flat-band voltage (V_{fb}) and the interface trap density (D_{it}), for high- k dielectric films to be adopted as gate dielectrics of MOS devices. The V_{fb} is a critical parameter in selecting the device operation conditions, and a low D_{it} is crucial for high-speed operation. Unfortunately, the parameters of high- k films are usually inferior to those of conventional SiO_2 because of the high interface and bulk defect densities.^{7–9}

In this study, an Al_2O_3 layer grown by the ALD technique was selected as the RBL because of its large band gap,

^{a)}Electronic mail: cheolsh@plaza.snu.ac.kr

amorphous nature, and reasonably high dielectric constant (9–10). In addition, the ALD process for the Al_2O_3 film growth is fairly mature at the moment due to its adoption as a capacitor dielectric in dynamic random access memory (DRAM).¹⁰ Process maturity is another critical factor that should be considered.

In this article, the thermal stability of the structural and electrical performance of $\text{HfO}_2/\text{Al}_2\text{O}_3$ gate dielectric stacks, such as the EOT and V_{fb} , was studied in detail as a function of the postannealing temperature. In particular, structural changes in the $\text{HfO}_2/\text{Al}_2\text{O}_3$ gate dielectric stacks were studied using high-resolution transmission electron microscopy and x-ray photoelectron spectroscopy, and the results were compared with the electrical characterization results, such as changes in the EOT and V_{fb} . For a more detailed understanding of the changes, the structural alterations of single layers, HfO_2 and Al_2O_3 layers, respectively, were also examined after annealing at similar conditions.

II. EXPERIMENTAL PROCEDURES

HfO_2 thin films were deposited by the ALD technique using a traveling wave-type ALD reactor (Plus-200, Ever-tek Co.), which can process two 200-mm-diam wafers simultaneously. HfCl_4 and H_2O were used as the precursor and oxidant, respectively. The wafer temperatures were set to 300 and 400 °C during deposition. HfO_2 films were grown for 15 and 20 cycles at 300 and 400 °C, respectively, to make the film thicknesses similar. The thickness nonuniformity [(max–min)/2 average] was <3%. Details of the deposition process are reported elsewhere.⁶ The Al_2O_3 films were grown by another 200-mm-diam ALD system using trimethylaluminum [$\text{Al}(\text{CH}_3)_3$] (TMA) and O_3 as the precursor and oxidant, respectively, at a wafer temperature of 400 °C. The thickness nonuniformity [(max–min)/2 average] was <2%. The native oxide on the Si wafer surface was removed by Radio Corporation of America (RCA) cleaning immediately prior to Al_2O_3 film growth. Postannealing of the samples was performed with a vertical fused-silica tube furnace at temperatures ranging from 400 to 1000 °C for 10 min under pure N_2 atmosphere (O_2 concentration < 1 ppm).

The film thicknesses were measured by ellipsometry and cross-sectional high-resolution transmission electron microscopy (HRTEM) (JEOL JEM-3000F) equipped with a field-emission electron gun. Ten HRTEM pictures were taken of each sample to compensate for the error in film thickness measurement due to local variations. X-ray photoelectron spectroscopy (XPS) was used to characterize the structural changes. The characteristic x ray of Mg $K\alpha$ with photon energy of 1253.6 eV was used for XPS. The overall energy resolution was approximately 1 eV.

For electrical characterization, metal–insulator–semiconductor capacitors (MISCAPs) were fabricated by depositing Pt top electrodes through a shadow mask using an electron beam evaporation method. The accurate electrode area of each capacitor was measured using optical microscopy. The back side of the wafer was HF cleaned with Al metallization subsequently applied. Postmetallization annealing was performed at 400 °C for 30 min under 5% H_2

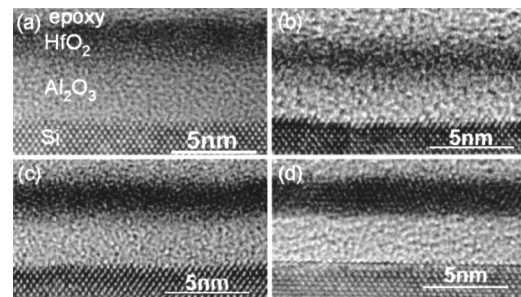


FIG. 1. HRTEM pictures of the $\text{HfO}_2/\text{Al}_2\text{O}_3$ film stack (a) in the as-deposited state and after annealing at (b) 650, (c) 900, and (d) 1000 °C, respectively.

+ 95% N_2 atmosphere to stabilize the electrical properties. A Hewlett-Packard 4194A impedance meter and a 4140B picoammeter were used for the capacitance versus voltage (C – V) measurements and leakage-current density versus voltage (J – V) measurements, respectively. Since the samples showed little frequency dispersion, the C – V measurement frequency was fixed at 1 MHz. The EOT of the film was calculated by C – V curve fitting taking into consideration the quantum-mechanical effect.¹¹

III. RESULTS AND DISCUSSION

A. Structural analysis of the films by HRTEM and XPS

1. High-resolution transmission electron microscopy

Figures 1(a)–1(d) show representative HRTEM pictures of the $\text{HfO}_2/\text{Al}_2\text{O}_3$ film stack in the as-deposited state and after annealing at 650, 900, and 1000 °C, respectively. Here, the HfO_2 film was grown at 300 °C for 15 cycles. The as-grown HfO_2 and Al_2O_3 film thicknesses were 2.6 and 3.3 nm, respectively. It should be noted that the as-grown HfO_2 and Al_2O_3 films have an amorphous structure. Crystallization of the Al_2O_3 RBL does not occur even after annealing at 1000 °C, whereas crystallization of the HfO_2 film does occur. The crystallized upper layer (UL) was HfAl_xO_y , as shown by the XPS results shown in Fig. 5. The variations in thickness of the Al_2O_3 RBL, HfO_2 , and the total layers as a function of the postannealing temperature are shown in Fig. 2. They all show minimum values at approximately 650 °C

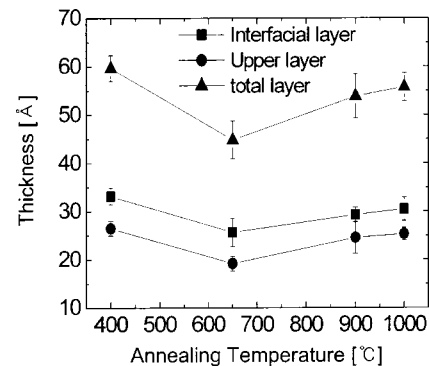


FIG. 2. Variations in the thickness of the Al_2O_3 RBL, HfO_2 , and total layers.

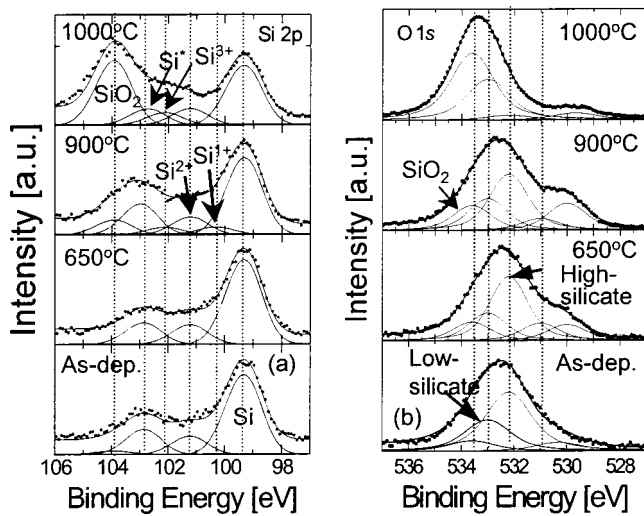


FIG. 3. XPS results of (a) Si 2*p* and (b) O 1*s* in Al₂O₃ film after annealing at various temperatures.

and increase with an increase in postannealing temperature. The decrease in thickness with an increase in annealing temperature up to 650 °C might be due to the effect of densification and the removal of impurities, such as Cl, from the films. There was a big decrease in the Cl concentration with increase in postannealing temperature in the secondary ion mass spectroscopy (SIMS) analysis results (not shown here). The increase in thickness with an increase in postannealing temperature >650 °C may arise from Si oxidation by residual oxygen and intermixing between the two layers, as shown in the XPS results in Figs. 3–5.

2. X-ray photoelectron spectroscopy

The structural and compositional changes of the HfO₂/Al₂O₃ film stack according to the annealing temperature were investigated using XPS. For better understanding of the changes that take place during annealing, the varia-

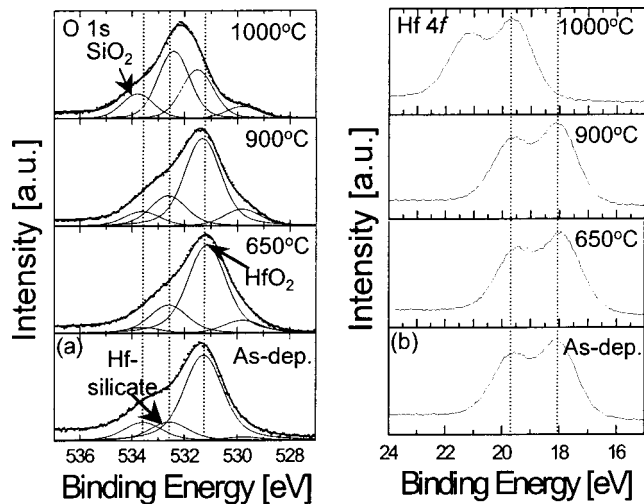


FIG. 4. XPS results of (a) O 1*s* and (b) Hf 4*f* in HfO₂ film after annealing at various temperatures.

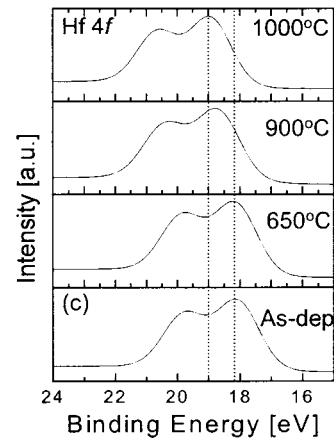
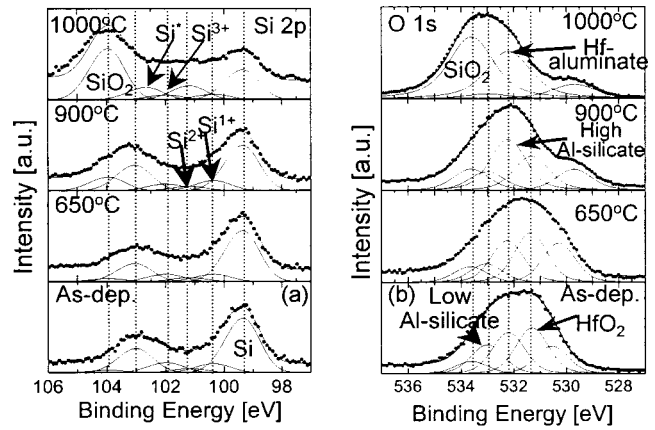


FIG. 5. XPS results of (a) Si 2*p*, (b) O 1*s*, and (c) Hf 4*f* in HfO₂/Al₂O₃ film after annealing at various temperatures.

tions in the Al₂O₃ and HfO₂ single layers grown under the same conditions as the films in the HfO₂/Al₂O₃ film stack were also investigated.

a. XPS of Al₂O₃/Si. First, the XPS results showing the variations in the Al₂O₃ films as a function of the annealing temperature are discussed. Figures 3(a) and 3(b) show the variations in XPS peak intensity and position of the Si 2*p* and O 1*s* peaks of the 5-nm-thick Al₂O₃ film as a function of the annealing temperature, respectively. The dots and the lines represent the experimental data and the simulation results, respectively, after curve fitting by decomposition. Figure 3 shows the excellent match between the experimental data and the simulation results.

The Si 2*p* core level XPS spectra were composed of five different component peaks at binding energies of 99.3, 100.2, 101.2, 102.1, 102.9, and 103.9 eV, respectively. The peak at 99.3 eV was assigned to the Si substrate (0 oxidation state) peak and the relative shifts in energy of each peak are summarized in Table I along with data reported in recent literature.^{12–14} Many intermediate oxidation states (corresponding to 1+, 2+, 3+, and silicate) of Si ions have been reported^{12,13} in addition to fully oxidized SiO₂ (4+). First, these data were compared to literature values; the shifts in energy of Si¹⁺ and Si²⁺ in this study are similar to the values in the literature.¹² For the Si⁴⁺ peak position, the difference in the shift in energy was quite serious, 3.67 (Ref. 12) ~3.86 (Ref. 13) vs 4.60. This might be due to the fact

TABLE I. Shift in energy observed for each Si oxidation state of SiO₂ and silicate.

	Energy shift (eV), [Peak position (eV)]			
	0.6 nm SiO ₂ ^a	0.7 nm HfO ₂ / 0.7 nm SiO ₂ ^b	Al ₂ O ₃ /Si	HfO ₂ /Al ₂ O ₃ /Si
Si ¹⁺	1.00	0.94	0.9, (100.2)	1.0, (100.3)
Si ²⁺	1.82	1.83	1.9, (101.2)	1.9, (101.2)
Si ³⁺	2.62	2.56	2.8, (102.1)	2.7, (102.0)
Si*		3.16	3.6–3.7, (102.9–103.0)	3.7, (103.0)
Si ⁴⁺	3.67	3.86	4.6, (103.9)	4.6, (103.9)

^aReference 12.^bReference 13.

that the data from the literature in Table I were from ultrathin SiO₂ (0.6–0.7 nm) where the SiO₂ structure was incomplete. The SiO₂ peak position in this study, ~103.9 eV, was similar to the value (103.7 eV) of thicker SiO₂ (>3 nm) reported by Keister *et al.*¹⁴ In this study, the interfacial SiO₂ was believed to be at least 1 nm thick and the SiO₂ structure more bulk like. The shift in energy of Si³⁺ was larger than reported values by approximately 0.18–0.24 eV, which is believed to be due to the larger SiO₂ thickness. The peak denoted Si* may originate from the Al-silicate with high Al concentration (high silicate). Renault *et al.*¹³ also assigned a similar peak in their 0.7 nm HfO₂/0.7 nm SiO₂ sample to the Hf-silicate peak. The present samples (Al₂O₃/Si, HfO₂/Si, and HfO₂/Al₂O₃/Si) also showed similar peaks at a shift of binding energy of 3.6–3.7 eV. Suboxide peaks are observed in the ultrathin SiO₂ films and are known to originate in the SiO₂/Si interface region where the oxygen is deficient.^{12–14}

It was reported that rather serious Si diffusion occurs during Al₂O₃ ALD on Si and results in the formation of an Al-silicate layer.¹⁵ Crivelli *et al.*¹⁵ reported double-layer structures composed of Al-rich and Si-rich layers using Rutherford back scattering spectroscopy (RBS) experiments on 3–4-nm-thick ALD Al₂O₃ films.

The O 1s signals in Fig. 3(b) further help in understanding layered structures. It was found that the O signals are composed of four components whose peak positions are 530.9, 532.1, 533.0, and 533.6 eV, respectively. From a comparison with reference data,¹⁶ it is reasonable to assign the peak at 533.6 eV to SiO₂. It is reasonable to assign the peak at 532.1 eV to high Al concentration Al silicates (high silicate). The typical O 1s peak position of stoichiometric Al₂O₃ is around 531.0 eV.¹⁶ Therefore, the peak at 533.0 eV should be assigned to the low Al-concentration silicate. The absence of the O 1s peak at 531 eV suggests that there is almost no pure Al₂O₃ layer. Actually, the dielectric constant of the present Al₂O₃ film measured by high-frequency C–V was only 7.6,¹⁷ which again supports silicate formation. The remaining two peaks at lower binding energies might have originated from surface contamination.

The change in film structure with the annealing temperature can be understood from the relative variations in intensity of each peak. The as-deposited film appears to consist of a high silicate on top, a low-silicate underlayer, and an ultrathin SiO₂ layer at the interface. It is clear that the SiO₂ layer grew monotonically at the film/substrate interface because of the residual oxygen diffusion towards the interface from

variations in both the Si⁴⁺ peak and the O 1s peak at 533.6 eV with the annealing temperature. This certainly decreases the density of the capacitance of the film. Interesting observations are seen from the Si and O peaks of silicate layers. The Si* peak intensity increases with the annealing temperature up to 900 °C then decreases at 1000 °C. The Si* peak position shifts toward lower binding energy by approximately 0.2 eV, suggesting that the Al concentration of the remaining high silicate increases after annealing at 1000 °C. It appears that the high-silicate layer was rather stable up to 900 °C with only a slight increase in the Si concentration due to Si diffusion. During annealing at 1000 °C, the high silicate converts into low silicate due to serious Si diffusion from the underlayers and oxygen diffusion from the atmosphere. Some Al ions concurrently segregate towards the surface, resulting in a residual high silicate with higher Al concentration as suggested by the variations in Si* peak intensity and position. The Si 2p peaks from the low silicate might have overlapped another Si 2p peak (probably Si⁴⁺). A thick SiO₂ layer grew concurrently at the interface during annealing at 1000 °C. The sudden change in film structure at 1000 °C is further confirmed by the behavior of the Al 2p peaks. It was observed that the Al 2p peak position gradually shifted towards higher binding energy at annealing temperatures up to 900 °C, and that there was a sudden increase in the shift after annealing at 1000 °C. The shift after annealing at 1000 °C was 1.36 eV. The results were compared with those of HfO₂/Al₂O₃/Si.

b. XPS of HfO₂/Si. Next, the variations in XPS of HfO₂ films are discussed. Figures 4(a) and 4(b) show the variations in XPS peak intensity and position, respectively, of the O 1s and Hf 4f peaks of the 5-nm-thick HfO₂ film as a function of the annealing temperature.

The O 1s peak was composed of four peaks where the peak positions were 529.7, 531.3, 532.6, and 533.6 eV, respectively, in the as-deposited state. It is reasonable to assign the peaks at 531.3, 532.6, and 533.6 eV to the O 1s peak of HfO₂ (that contains a small amount of Si), Hf silicate, and SiO₂, respectively. It should be noted that the binding energy of the Hf-silicate O 1s peak is ~0.6 eV smaller than that of the low-concentration Al-silicate O 1s peak (~533.0 eV). The peak at 529.7 eV might have originated from surface adsorbed oxygen.

The as-deposited film appears to be composed mainly of HfO₂ and Hf silicate and SiO₂. The extent of SiO₂ formation

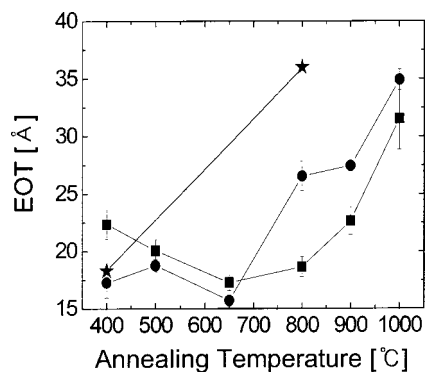


FIG. 6. EOTs of stacked dielectric films as a function of the postannealing temperature. The HfO_2 films were grown at 300 (square symbols) and 400 °C (circle symbols), respectively. Stars correspond to HfO_2 without an Al_2O_3 layer.

is greater than that of $\text{Al}_2\text{O}_3/\text{Si}$ probably due to the smaller energy of formation of HfO_2 compared to Al_2O_3 . This corresponds well to the HRTEM and electrical measurement results in which the dielectric constant of the interfacial layer corresponded to that of a Si-rich Hf silicate.^{5,6} As the annealing temperature increases, the interfacial SiO_2 grew monotonically, confirming again the validity of the electrical measurement results for a decrease in density of the capacitance with an increase in annealing temperature (Fig. 6).

Interesting observations can be seen in the variations in Hf-silicate and HfO_2 peaks with an increase in annealing temperature. The O 1s peak intensity corresponding to HfO_2 is rather constant up to 900 °C but suddenly decreases at 1000 °C, whereas the O 1s peak intensity corresponding to Hf-silicate suddenly increases at 1000 °C. This suggests that the structural change in the HfO_2/Si system is interfacial SiO_2 growth while retaining the $\text{HfO}_2 + \text{Si}$ -rich Hf-silicate structure in the main body of the film up to 900 °C. HRTEM showed that the HfO_2 and Hf silicate are crystallized and mixed within a single layer rather than forming a double layered structure.⁶ It should be noted that the HfO_2 and Hf silicate lattice fringes were hardly discernable by HRTEM due to the large number and similarity of the lattice spacing of the two phases.⁶ However, at 1000 °C, the HfO_2 reacts with diffused Si, O, and Hf silicate and forms Hf silicate with a medium Hf concentration, as suggested by the sudden increase in the O 1s peak corresponding to Hf silicate and the decrease in the O 1s peak corresponding to HfO_2 . Furthermore, the peak position of the O 1s peak corresponding to Hf silicate moved toward lower binding energy, suggesting an increase in the Hf concentration of this material. In addition, the peak position of the O 1s peak corresponding to HfO_2 moved toward higher binding energy, suggesting an increase in the Si concentration in the remaining HfO_2 .

Figure 4(b) shows the variation in Hf 4f peak as a function of the annealing temperature. It can again be confirmed that there was a sudden change in the Hf bonding status at 1000 °C due to the large formation of Hf silicate.

c. XPS of $\text{HfO}_2/\text{Al}_2\text{O}_3/\text{Si}$. Finally, the variations in the XPS results for the $\text{HfO}_2/\text{Al}_2\text{O}_3$ stacked films are discussed. Figures 5(a) and 5(b) show the variations in XPS peak inten-

sity and position of the Si 2p and O 1s peaks, respectively, of the film shown in Fig. 2, as a function of the annealing temperature. The Si 2p spectra of this sample up to 900 °C are almost identical to those of $\text{Al}_2\text{O}_3/\text{Si}$, suggesting that the HfO_2 overlayer did not affect the underlying Al_2O_3 structure. The behavior of the Si 2p peak corresponding to SiO_2 is very similar to that of $\text{Al}_2\text{O}_3/\text{Si}$. The variations in O 1s peak corresponding to that of the high-Al silicate (532.3 eV) and SiO_2 (533.6 eV) are also similar to that of $\text{Al}_2\text{O}_3/\text{Si}$. However, the O 1s peak corresponding to the low-Al silicate (533.1 eV) show somewhat different behavior from that of the $\text{Al}_2\text{O}_3/\text{Si}$. Its intensity decreases monotonically with an increase in annealing temperature and almost completely disappears at 1000 °C. It should be noted that the O 1s peak corresponding to the low silicate increased at this temperature for the $\text{Al}_2\text{O}_3/\text{Si}$ case. The Si 2p and O 1s peak intensities corresponding to SiO_2 largely increase and the Si* peak position shifts toward lower binding energy by 0.2 eV at this temperature, similar to in the $\text{Al}_2\text{O}_3/\text{Si}$ case. SiO_2 formation during annealing at 1000 °C appears to be even more serious than in the case of $\text{Al}_2\text{O}_3/\text{Si}$ although there was a thin HfO_2 overlayer on top of the Al_2O_3 . This might be due to the catalytic effect of oxygen molecule dissociation of HfO_2 .¹⁸ This suggests that Al ions in the high- and low-silicate layers segregate towards the overlying HfO_2 layer, leaving thick SiO_2 and very thin high silicate with a higher Al-concentration layer under the HfO_2 layer. This hypothesis can be confirmed by the following observations.

Other interesting results can be found from variation of the O 1s peak corresponding to the HfO_2 (~531.4 eV). This peak remained up to 900 °C but completely disappeared after annealing at 1000 °C as a result of the formation of either Hf silicate or Hf aluminate. Therefore, the rather large O 1s peak observed at 532.3 eV after annealing at 1000 °C might be due either to Hf silicate or Hf aluminate. The observed peak position of Hf silicate in the HfO_2/Si sample was approximately 532.6 eV. Therefore, the large peak observed at 532.3 eV can be assigned as a Hf-aluminate peak. Furthermore, the almost complete disappearance of the Al silicate after annealing at 1000 °C suggests that Al ions from the high and low silicates were absorbed by HfO_2 and formed Hf aluminate at this temperature. The slightly larger peak width (full width half maximum) of the O 1s peak at 532.3 eV after annealing at 1000 °C compared to those at lower temperatures suggests that the peak might be composed of overlapping Hf aluminate and residual high Al-concentration Al silicate. Further confirmation of Hf-aluminate formation is given by the shift of the Hf 4f peak at 1000 °C, shown in Fig. 5(c), where the shift in energy from the as-deposited state is only 0.86 eV whereas that for Hf-silicate formation it was 1.55 eV [Fig. 4(b)]. Figure 5(c) also shows that interfacial reaction between Al_2O_3 and HfO_2 does not occur up to 650 °C by the nonvarying Hf 4f peak position up to this temperature. Intermixing appears to begin at 900 °C. The Hf aluminate has a crystalline structure as shown in the HRTEM picture in Fig. 1(d). Both the Si 2p and O 1s peaks consistently show a monotonic increase of SiO_2 formation with an increase in annealing temperature up to 1000 °C. This might be due to oxidation of the Si surface by residual oxygen, and

it may constitute the major reason for the increasing EOT at temperatures higher than 650 °C, as shown in Fig. 6.

B. Electrical characterization

Information regarding the changes in thickness of each layer (HRTEM pictures in Figs. 1 and 2) and the structural change (XPS results in Fig. 5) offers a more detailed understanding of the variations in EOT in Fig. 6 and V_{fb} in Fig. 7 of stacked films as a function of the annealing temperature. Because the physical thickness of each layer is known from HRTEM, the EOT of each layer can be estimated if the dielectric constants (ϵ_r) of the layers are known. The fixed charge densities (Q_f) can also be determined from estimates of EOT and V_{fb} .

1. Equivalent oxide thicknesses

Figure 6 shows the variations in EOT values of stacked dielectric films as a function of the postannealing temperature for HfO₂ films grown at 300 and 400 °C, respectively. For a fairer comparison, the number of deposition cycles was increased for the HfO₂ film deposited at 400 °C in order to produce similar film thickness to that deposited at 300 °C due to the decrease in HfO₂ film growth rate at 400 °C.⁶ The EOT values of a HfO₂ film, grown at 300 °C, without the Al₂O₃ RBL in the as-deposited state and after the postannealing stage at 800 °C, are also included in Fig. 6 for comparison. It can be understood that the adoption of an Al₂O₃ RBL is to a certain degree effective in improving the thermal stability of the EOT.

It can be understood that variations in EOT values almost exactly follow the variation in total film thickness with an increase in postannealing temperature from a comparison between Figs. 2 and 6. Both stacked films show minimum EOT values (1.6–1.8 nm) at around 650 °C, which then increase with the annealing temperature. However, it should also be noted that the EOT values of the films annealed at temperatures >900 °C are larger than that of the film annealed below 650 °C even though their physical thickness is smaller (Fig. 2). This can be explained by variations in the film composition and the formation of SiO₂ at the Si interface that occur during high temperature annealing.

For the films shown in Fig. 2, i.e., when the HfO₂ film was grown at 300 °C, the interlayer (IL) and UL thicknesses are 3.3 and 2.6 nm, respectively, after annealing at 400 °C. The estimated EOT of the IL is 1.8 nm when the ϵ_r of the IL is assumed to be 7 from the separately measured dielectric constant of the 6-nm-thick Al₂O₃ layer (7–7.5) grown under the same conditions. It was also assumed that the IL at 400 °C is composed of an Al-silicate layer ($\epsilon_r=7$) since the formation of interfacial SiO₂ was negligible at this stage according to XPS. Actually, it might be more reasonable to assume that the IL is composed of ultrathin SiO₂ ($\ll 0.5$ nm) and Al silicate with higher ϵ_r (>7). However, since the interfacial SiO₂ thickness cannot be estimated separately in this experiment, the IL is considered a single layer with ϵ_r of 7. The EOT of the UL of the film annealed at 400 °C must be 0.4 nm since the total measured EOT was 2.2 nm (2.2–1.8 nm). Therefore, the ϵ_r of the UL should be 26 according to the measured physical thickness of 2.6 nm. If ϵ_r of the IL

were assumed to be slightly larger, i.e., 7.5, then ϵ_r of the UL would become 21. This (21–26) is a reasonable dielectric constant for a thin HfO₂ film.

For the film annealed at 650 °C, the estimated EOTs of the IL and UL were 1.5 and 0.3 nm, respectively, and the estimated ϵ_r of the UL was 24, according to the thicknesses of each layer. Here, ϵ_r of the IL was also assumed to be 7 considering there was little change in the XPS results of the IL.

For the film annealed at 900 °C, the IL was considered to be composed of 0.8-nm-thick interfacial SiO₂, considering the appearance of the strong SiO₂ signal in XPS, and a 2.0-nm-thick Al-silicate layer with ϵ_r of 7 [2.8 nm (total IL thickness) and –0.8 nm (SiO₂ thickness)]. Here, the thickness of the interfacial SiO₂ layer (0.8 nm) was estimated from separate measurement of the increase in thickness in the Al₂O₃ film after annealing under similar conditions. The reason for the smaller increase in IL thickness in these experiments (0.2–0.3 nm) is the absorption of some Al silicate by the upper-lying HfO₂ that forms Hf aluminate, as seen in Fig. 5. Therefore, the EOT of the Al-silicate layer should be 1.1 nm, and the EOT and ϵ_r of the UL are 0.4 nm and 23, respectively, according to the total EOT and physical thickness of the UL (2.3 nm) at this temperature. Here, the EOTs of interfacial SiO₂ and Al silicate were estimated separately because this is essential in understanding the V_{fb} behavior.

For the film annealed at 1000 °C, it should be noted that there was a sudden change in film structure at this temperature. The IL became almost SiO₂ with a small amount of residual Al silicate and the UL transformed into Hf aluminate. Since HRTEM could not resolve the SiO₂ and residual Al silicate, the IL was considered to be SiO₂ with a low Al concentration that has ϵ_r of 4.5–5. The EOT of the IL was then estimated to be 2.6–2.3 nm from the physical thickness of 3.0 nm. Therefore, the EOT and ϵ_r of the UL should be 0.6–0.8 nm and 16–13, respectively. The ϵ_r of 16–13 appears to be reasonable as a dielectric constant of a crystallized thin Hf-aluminate film. We actually measured the dielectric constant of Hf-aluminate films grown by chemical vapor deposition using a metalorganic precursor that contained Hf and Al, and found that the ϵ_r of the grown Hf-aluminate films ranged from 10 to 20 depending on the film composition.¹⁹

The physical thicknesses, the assumed and calculated ϵ_r , the estimated EOTs of the IL (and interfacial SiO₂), and the UL of the films annealed at various temperatures are summarized in Table II. The estimated values in Table II seem to be reasonable considering the reasonable ϵ_r value of the UL and its variations as a function of the annealing temperature. The Si and Al concentrations in the UL increase with an increase in annealing temperature, shown in the XPS results in Fig. 5, so ϵ_r of the HfO₂ layer (UL) should decrease gradually up to 900 °C and then suddenly decrease at 1000 °C due to the almost complete transformation to Hf aluminate. In addition, the decrease in ϵ_r of the UL must be counteracted by the densification effect of the UL as a result of the high temperature heat treatment. Therefore, the decrease should be minimized provided the UL remains HfO₂ or Hf silicate. This fits very well to the estimates made

TABLE II. Thickness, EOT, and ϵ_r of the IL and UL after annealing at various temperatures. The estimated error in EOT is approximately ± 0.05 nm. The estimated error in V_{fb} is approximately 5%–10% due to uncertainty in the Pt workfunction and variation of $C-V$.

Temperature (°C)	Interlayer			Upper layer			EOT* (nm)	V_{fb}^c (V)	V_{fb}^m (V)
	Thickness (nm)	EOT (nm)	ϵ_r	Thickness (nm)	EOT (nm)	ϵ_r			
400	3.3	1.8–1.7	7–7.5	2.6	0.4–0.0	26–21	2.1	0.78	0.78
650	2.6	1.5	7	2.0	0.3	24	1.7	0.61	0.83
	2.8	1.9							
900	(0.8+2.0)	(0.8+1.1)	3.9; 7	2.3	0.4	23	1.5	0.56	0.48
1000	3.0	2.6–2.3	4.5–5	2.6	0.8–0.6	13–16	0.8–0.6	0.31–0.21	0.79

above. From these calculations, the V_{fb} behavior as a function of the annealing temperature, shown in Fig. 7, was interpreted.

2. Flat-band voltage and fixed charge density

Figure 7 shows the variation in V_{fb} and hysteresis voltage (V_{hy}) in $C-V$ measurements as a function of the post-annealing temperature. Here, HfO_2 films were grown at 300 °C and a $C-V$ measurement bias was applied from the accumulation (–3 V) to the depletion (+2 V) regions and returned to the accumulation (–3 V) region. The very small V_{hy} values (<20 mV) suggest that charge capturing of the stack films was minimized. The V_{fb} due to the mismatch in workfunction between the Pt top electrode and Si substrate is approximately 0.6 V. Therefore, V_{fb} due to interfacial fixed charge should be the V_{fb} in Fig. 7 –0.6 V. These values are included in the right-hand column of Table II, denoted V_{fb}^m .

Johnson *et al.*⁷ reported that the Al_2O_3/SiO_2 interface has negative Q_f and density as high as $8 \times 10^{12} \text{ cm}^{-2}$. The reason for Q_f at the Al_2O_3/SiO_2 interface is that negatively charged Al^{3+} ions with tetrahedral coordination are in contact with O atoms of interfacial SiO_2 .⁷ Crivelli *et al.*¹⁵ also reported similar negative fixed charge density at the Al_2O_3/SiO_2 interface. The Q_f induces a shift in flat-band voltage (V_{fb}) of the gate electrode through capacitive coupling of the gate dielectric, which adversely affects CMOS field effect transistor (FET) operation (a shift in the threshold

voltage). Therefore, Q_f should be reduced to that of the SiO_2/Si or be compensated for by countercharges.

For these stacked films, there are three interfaces that have Q_f 's: SiO_2/Si , Al_2O_3 (or Al-silicate)/ SiO_2 , and HfO_2 (or Hf-silicate, Hf-aluminate)/ Al_2O_3 (or Al-silicate) interfaces. The Q_f of the SiO_2/Si interface is usually quite low (a few 10^{10} cm^{-2}), which produces negligible V_{fb} in the gate electrode.²⁰ For example, if there is a fixed charge density of $5 \times 10^{10} \text{ cm}^{-2}$ at the SiO_2/Si interface and the total EOT of the dielectric stack is 3.0 nm, then the V_{fb} due to this charge is only 0.007 V, which is a negligible compared to the V_{fb}^m . It has also been noted that the Q_f of the HfO_2 (or Hf-silicate)/ Al_2O_3 (or Al-silicate) interface is smaller than that of the Al_2O_3 (or Al-silicate)/ SiO_2 interface by an order of magnitude.²¹ Furthermore, the large capacitance of the UL makes the V_{fb} due to the Q_f of the HfO_2 (or Hf-silicate)/ Al_2O_3 (or Al-silicate) interface smaller. For example, $8 \times 10^{11} \text{ cm}^{-2}$ of negative fixed charge with UL capacitance and an EOT of 0.4 nm induced V_{fb} of only 0.015 V, which is also a negligible compared to the V_{fb}^m here. Therefore, the Q_f of the Al_2O_3 (or Al-silicate)/ SiO_2 interface should be noted.

Because the EOTs of each layer are known, the capacitances responsible for V_{fb} can be calculated under the assumption that the Al_2O_3 (or Al-silicate)/ SiO_2 interface has negative Q_f of $8 \times 10^{12} \text{ cm}^{-2}$.⁷ For example, the V_{fb} of the sample annealed at 900 °C due to Q_f of $8 \times 10^{12} \text{ cm}^{-2}$ at the Al_2O_3 (or Al-silicate)/ SiO_2 interface, as a result of capacitance with an EOT of 1.5 nm [1.1 nm (Al silicate) + 0.4 nm (UL)], is 0.56 V. The calculated V_{fb} values (V_{fb}^c) of the samples annealed at various temperatures due to the assumed Q_f of $8 \times 10^{12} \text{ cm}^{-2}$ at the Al_2O_3 (or Al-silicate)/ SiO_2 interface are included in the eighth column of Table II. The seventh column of Table II shows the corresponding EOTs of the capacitors (EOT*) that produce the V_{fb} at each temperature when the Q_f is assumed to be constant irrespective of the annealing temperature. For 400 and 650 °C, the interfacial SiO_2 thickness was arbitrarily taken to be 0.1 nm, and the EOT* was taken as the total EOT –0.1 nm.

The excellent coincidence between V_{fb}^c and V_{fb}^m after annealing at 400 °C shows that the present analysis is quite reasonable. The larger V_{fb}^m compared to the V_{fb}^c at 650 °C suggests that Q_{fb} at the interface increases. The smaller V_{fb}^m compared to the V_{fb}^c at 900 °C suggests that Q_{fb} at the interface decreases as a result of the thermal annealing effect. The similar decrease in Q_f of the Al_2O_3 (or Al-silicate)/ SiO_2 in-

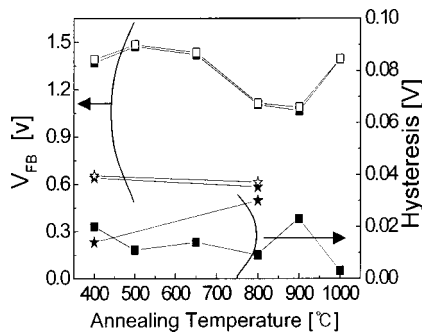


FIG. 7. Variation in the shift in flat-band voltage (V_{fb}) and hysteresis voltage (V_{hy}) in $C-V$ measurements of HfO_2/Al_2O_3 film as a function of the postannealing temperature. Square symbols correspond to HfO_2/Al_2O_3 and stars correspond to HfO_2 without an Al_2O_3 layer. Closed and open symbols correspond to voltage sweeps from –3 to +2 and from +2 to –3 V, respectively.

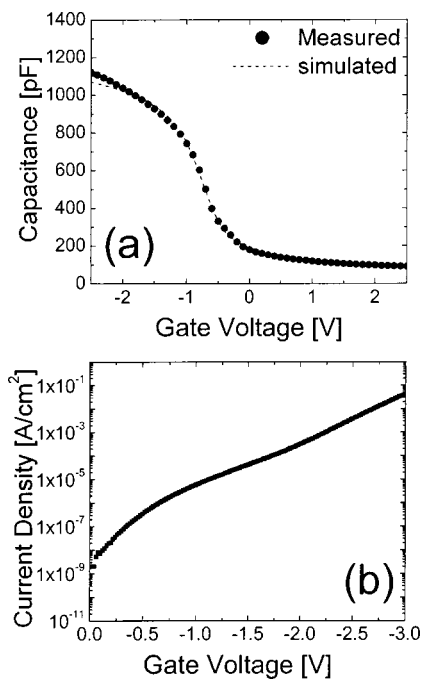


FIG. 8. (a) C - V and (b) J - V curves of a 4-nm-thick $\text{HfO}_2/\text{Al}_2\text{O}_3$ film stack with a poly-Si gate electrode after annealing at 1000°C for 10 s.

interface was also reported by Crivelli *et al.*¹⁵ after annealing at the same temperature. A quite noticeable change in V_{fb} is found in the sample annealed at 1000°C . The V_{fb}^m again increases, rather than decreases, which suggests that Q_f increases due to annealing at 1000°C . Since the IL became almost SiO_2 and the UL was Hf aluminate at this temperature, the interface between the SiO_2 and Hf aluminate should have negative Q_f density as high as $2.4 \times 10^{13} \text{ cm}^{-2}$ when the EOT* is arbitrarily taken as 0.7 nm (Table II). The structural incompatibility between the amorphous SiO_2 (or low Al-concentration Al silicate) and crystalline Hf aluminate may constitute the reason for such an extremely high Q_f .

Figure 8 shows the C - V curve of a 4-nm-thick $\text{HfO}_2/\text{Al}_2\text{O}_3$ stacked film. For this specific case, the gate electrode was composed of heavily doped poly-Si (doping concentration of $5 \times 10^{19} \text{ cm}^{-3}$). The film was postannealed at 950°C for 30 s before poly-Si gate deposition to allow densification and at 1000°C for 10 s under N_2 atmosphere to activate the dopant in the gate electrode. The EOT value of this dielectric, estimated from C - V curve fitting (shown in Fig. 8) and taking into account the quantum-mechanical and poly-Si carrier depletion effects, was 1.3 nm. The leakage current density of the film at -1 V (shown in the inset of Fig. 8) is $8 \times 10^{-6} \text{ A/cm}^2$, which is approximately 10^7 times smaller than that of SiO_2 with similar EOT. Therefore, the present $\text{HfO}_2/\text{Al}_2\text{O}_3$ stacked film shows great promise as a gate insulator for future FETs.

IV. CONCLUSIONS

$\text{HfO}_2/\text{Al}_2\text{O}_3$ gate dielectric thin films stacks were deposited on Si wafers using the ALD technique. The adoption of an Al_2O_3 RBL suppresses Si diffusion to a certain degree during HfO_2 film deposition and postannealing. This results

in a smaller increase in the EOT values as a result of postannealing at temperatures $>650^\circ\text{C}$ compared to single layer- HfO_2 film on Si. The EOT values decrease with postannealing at temperatures $<650^\circ\text{C}$ by densification. The increase in the EOT with an increase in postannealing temperature ($>650^\circ\text{C}$) was due mainly to the formation of SiO_2 by residual oxygen in addition to variations in the total thickness and composition of the film stack. The RBL was composed of Al_2O_3 , Al silicate and interfacial SiO_2 .

There are critical differences in phase stability at 1000°C Al_2O_3 and HfO_2 single layers and $\text{HfO}_2/\text{Al}_2\text{O}_3$ double layers. Almost all of the Al_2O_3 layer (or high Al concentration Al silicate) reacted with Si and O and formed a medium Al concentration Al silicate. The formation of interfacial SiO_2 was serious. For the HfO_2 film, Hf silicate also formed, and the formation of interfacial SiO_2 was also serious. The HfO_2 layer on top of the Al_2O_3 layer absorbed Al during high temperature ($\sim 1000^\circ\text{C}$) annealing, resulting in a crystallized Hf aluminate with a small amount of Al silicate remaining. The formation of interfacial SiO_2 was as serious as that in the Al_2O_3 single layer.

The interface and bulk trapping properties of the charge carriers were generally acceptable but were further improved by postannealing. However, the rather high fixed charge density at the Al_2O_3 (or Al-silicate)/ SiO_2 interface induced a further shift in V_{fb} , which cannot be removed by postannealing. The structural incompatibility at the crystalline Hf-aluminate/ SiO_2 interface increased the fixed charge density to a very high level after annealing at 1000°C . A minimum EOT of 1.3 nm with very small leakage current density of $8 \times 10^{-6} \text{ A/cm}^2$ at -1 V was obtained from a capacitor with a poly-Si gate even after annealing at 1000°C for 10 s.

ACKNOWLEDGMENTS

This work was supported by the Korea Research Foundation (Grant No. KRF-2002-042-D00348), the Korean Ministry of Science and Technology through the National Research Laboratories Program, and by the National R&D Project for Nano Science and Technology (Grant No. M10214000097-02B1500-01500).

- ¹L. F. Schneemeyer, R. B. van Dover, and R. M. Fleming, *Appl. Phys. Lett.* **75**, 1967 (1999).
- ²S. J. Lee, H. F. Luan, W. P. Bai, C. H. Lee, T. S. Jeon, Y. Senzaki, D. Roberts, and D. L. Kwong, *Tech. Dig. - Int. Electron Devices Meet.* **2000**, 31.
- ³H.-J. Jung *et al.*, *Tech. Dig. - Int. Electron Devices Meet.* **2002**, 853.
- ⁴B. H. Lee *et al.*, *Tech. Dig. - Int. Electron Devices Meet.* **2000**, 39.
- ⁵B. K. Park, J. Park, M. Cho, C. S. Hwang, K. Oh, Y. Han, and D. Y. Yang, *Appl. Phys. Lett.* **80**, 2368 (2002).
- ⁶M. Cho, J. Park, H. B. Park, C. S. Hwang, J. Jeong, and K. S. Hyun, *Appl. Phys. Lett.* **81**, 334 (2002).
- ⁷R. S. Johnson, G. Lucovsky, and I. Baumvol, *J. Vac. Sci. Technol. A* **19**, 1353 (2001).
- ⁸G. D. Wilk, R. M. Wallace, and J. M. Anthony, *J. Appl. Phys.* **89**, 5243 (2001).
- ⁹I. S. Jeon, J. Park, D. Eom, C. S. Hwang, H. J. Kim, C. J. Park, H. Y. Cho, J.-H. Lee, N.-I. Lee, and H. K. Kang, *Appl. Phys. Lett.* **82**, 1066 (2003).
- ¹⁰W. S. Yang, Y. K. Kim, S. Y. Yang, J. H. Choi, H. S. Park, S. I. Lee, and J. B. Yoo, *Surf. Coat. Technol.* **131**, 79 (2000).
- ¹¹R. Clerc, B. De Salvo, G. Ghibaudo, G. Reimhold, and G. Pananakakis, *Solid-State Electron.* **46**, 407 (2002).
- ¹²J. H. Oh, H. W. Yeom, Y. Hagimoto, K. Ono, M. Oshima, N. Hirashita, M.

- Nywa, A. Toriumi, and A. Kakizaki, *Phys. Rev. B* **63**, 205310 (2001).
- ¹³O. Renault, D. Samour, J.-F. Damlencourt, D. Blin, F. Martin, S. Marthon, N. T. Barrett, and P. Besson, *Appl. Phys. Lett.* **81**, 3627 (2002).
- ¹⁴J. W. Keister, J. E. Rowe, J. J. Kolodziej, H. Niimi, H.-S. Tao, T. E. Madey, and G. Lucovsky, *J. Vac. Sci. Technol. A* **17**, 1250 (1999).
- ¹⁵B. Crivelli *et al.*, Symposium of the Materials Research Society, 2–6 December 2002, Boston, MA.
- ¹⁶J. F. Moulder, W. F. Stickle, P. E. Sobol, and K. D. Bomben, *Handbook of X-ray Photoelectron Spectroscopy* (Perkin-Elmer, Eden Prairie, MN, 1992), p. 45.
- ¹⁷I. S. Jeon, J. Park, D. Eom, C. S. Hwang, H. J. Kim, C. J. Park, H. Y. Cho, J.-H. Lee, N.-I. Lee and H. K. Kang, *Jpn. J. Appl. Phys., Part 1* **42**, 1222 (2003).
- ¹⁸Y. Hoshino, Y. Kido, K. Yamamoto, S. Hayashi, and M. Niwa, *Appl. Phys. Lett.* **81**, 2650 (2002).
- ¹⁹H. B. Park, J. Park, M. Cho, C. S. Hwang, S. J. Won, M. H. Park, and H. K. Kang, International Symposium on Integrated Ferroelectrics, 9–12 March 2003, Colorado Springs, CO.
- ²⁰T. Hori, *Gate Dielectrics and MOS ULSIs* (Springer, Berlin, 1997), p. 34.
- ²¹H. B. Park, M. Cho, J. Park, C. S. Hwang, J.-C. Lee, and S.-J. Oh *J. Appl. Phys.* **94**, 1898 (2003).